Thermal diffusivity of rods, tubes, and spheres by the flash method

Agustín Salazar[a] and Florencio Garrido
Departamento de Física Aplicada I, Escuela Técnica Superior de Ingeniería, Universidad del País Vasco, Alameda Urquijo s/n, 48013 Bilbao, Spain

Ricardo Celorrio
Departamento de Matemática Aplicada, Universidad de Zaragoza, Campus Río Ebro, Edificio Torres Quevedo, 50018 Zaragoza, Spain

(Received 26 December 2005; accepted 7 February 2006; published online 30 March 2006)

The flash method is the most used technique to measure the thermal diffusivity of solid samples. It consists of heating the front face of an opaque slab by a short light pulse and detecting the temperature evolution at its rear surface, from which the thermal diffusivity is obtained. In this paper, we extend the classical flash method to be used with rods, tubes, and spheres. First, the temperature evolution of the back surface of solid cylinders, hollow cylinders, and spheres is calculated. Then, experimental measurements of the thermal diffusivity on a set of stainless steel samples confirm the validity of the method. © *2006 American Institute of Physics*.
[DOI: 10.1063/1.2183584]

The flash method is the most acknowledged technique to measure the thermal diffusivity at high temperatures. In many countries, it is currently considered a standard for thermal diffusivity of solid materials. It was introduced by Parker and coworkers[1] and consists of heating the front face of an opaque slab by a short laser pulse and detecting the temperature evolution at its rear surface. The thermal diffusivity is obtained by measuring the time corresponding to the half maximum of the temperature rise ($t_{1/2}$), which is related to the thermal diffusivity through the expression: $t_{1/2}=0.1388L^2/D$, where L is the sample thickness and D is the thermal diffusivity. This procedure works under ideal conditions: negligible laser pulse duration and heat losses. When these requirements are not fulfilled, a fit to the complete temperature history of the rear surface must be performed.

In this paper, we extend the classical flash method to be used with nonplanar samples. In particular, solid cylinders, hollow cylinders, and spheres are studied. We proceed as follows. First, we calculate the temperature distribution when these samples are illuminated by a modulated light beam. The methodology used is based on the expansion in series of Bessel and Hankel functions of the thermal waves, which are generated at the sample surface. In this way, we obtain equivalent results to those found by Mandelis and coworkers using the Green's function method.[2,3] Then, starting from these modulated solutions, we calculate the temperature evolution of the sample after being heated by a short duration light pulse, by using the inverse Laplace transform.

Let us consider an infinite and opaque hollow cylinder with an outer radius a and an inner radius b, which is illuminated uniformly by a modulated light beam of intensity I_o and frequency f ($\omega=2\pi f$). Its cross section is shown in Fig. 1(a). The temperature oscillation at any point of the cylinder can be written as[4]

$$T(r,\phi,\omega)=\sum_{m=-\infty}^{\infty}A_m J_m(qr)e^{im\phi}+\sum_{m=-\infty}^{\infty}B_m H_m(qr)e^{im\phi}, \tag{1}$$

where $q=\sqrt{i\omega/D}$ is the thermal wave vector, and J_m and H_m are the mth order of the Bessel and Hankel functions of the first kind, respectively. The first term in Eq. (1) represents the ingoing cylindrical thermal wave starting at the sample surface, while the second one is the corresponding reflected wave at the inner surface. Equation (1) requires the knowledge of A_m and B_m that can be obtained from the heat flux continuity at the cylinder surfaces

$$K\left.\frac{\partial T}{\partial r}\right|_{r=a}+hT|_{r=a}=\frac{I_o}{2}\sum_{m=-\infty}^{\infty}\frac{(-i)^m}{\pi(1-m^2)}\cos\left(m\frac{\pi}{2}\right)e^{im\phi}, \tag{2a}$$

$$-K\left.\frac{\partial T}{\partial r}\right|_{r=b}+h'T|_{r=b}=0, \tag{2b}$$

where K is the thermal conductivity, and h and h' are the heat transfer coefficients at the outer and inner surfaces,

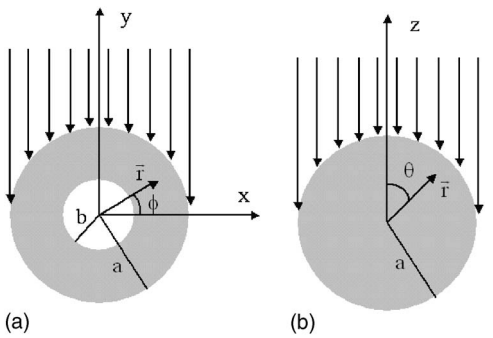

FIG. 1. Geometry of (a) a hollow cylinder and (b) a solid sphere.

[a]Electronic mail: agustin.salazar@ehu.es

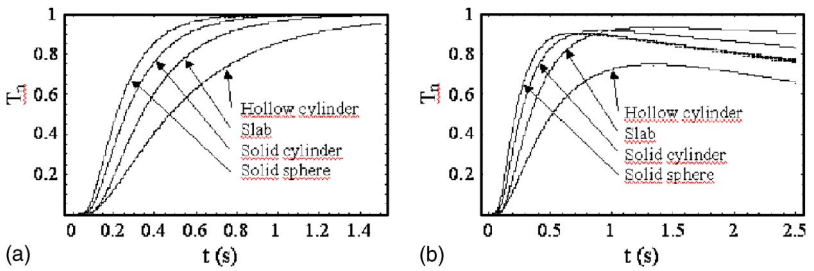

FIG. 2. Calculations of the normalized temperature rise at the rear side after the absorption of a Dirac light pulse. For a better comparison, the thickness of the slab and the diameter of the three other samples are taken to be equal (3 mm). The hollow cylinder has an inner diameter of 2 mm. (a) Negligible heat losses ($h=h'=0$). (b) Effect of heat losses ($h=200$ W m^{-2} K^{-1} and $h'=100$ W m^{-2} K^{-1}).

respectively, that include convective and radiative losses. The second member in Eq. (2a) represents the incident thermal flux, whose value is $(I_o \sin\phi)/2$ for $0 \leqslant \phi \leqslant \pi$ and zero for all other angles [see Fig. 1(a)], after being expanded in Fourier series. Substituting Eq. (1) into Eqs. (2), the temperature of the hollow cylinder is obtained

$$T(r,\phi,\omega)=\frac{I_o}{2Kq}\sum_{m=-\infty}^{\infty}\frac{(-i)^m}{\pi(1-m^2)}\cos\left(m\frac{\pi}{2}\right)e^{im\phi}\times\frac{[H'_m(qb)-R'H_m(qb)]J_m(qr)-[J'_m(qb)-R'J_m(qb)]H_m(qr)}{[J'_m(qa)+RJ_m(qa)][H'_m(qb)-R'H_m(qb)]-[J'_m(qb)-R'J_m(qb)][H'_m(qa)+RH_m(qa)]}, \tag{3}$$

where $R=h/Kq$, $R'=h'/Kq$, and J'_m and H'_m are the derivatives of the Bessel and Hankel functions, respectively. From Eq. (3), a simplified expression for a solid cylinder ($b=0$) is obtained:

$$T(r,\phi,\omega)=\frac{I_o}{2Kq}\sum_{m=-\infty}^{\infty}\frac{(-i)^m}{\pi(1-m^2)}\cos\left(m\frac{\pi}{2}\right)\times\frac{J_m(qr)e^{im\phi}}{J'_m(qa)+RJ_m(qa)}. \tag{4}$$

Now we consider an opaque sphere of radius a illuminated uniformly by a light beam of intensity I_o modulated at a frequency f. Its cross section is shown in Fig. 1(b). The temperature oscillation at any point of the sphere can be written as[5]

$$T(r,\theta,\omega)=\sum_{n=0}^{\infty}a_n j_n(qr)P_n(\cos\theta), \tag{5}$$

which represents a spherical thermal wave starting at the sample surface. Here j_n are the nth order of the spherical Bessel functions and P_n the Legendre polynomials. Equation (5) requires the knowledge of a_n that can be obtained from the heat flux continuity at the sphere surface

$$K\left.\frac{\partial T}{\partial r}\right|_{r=a}+hT|_{r=a}=\frac{I_o}{2}\sum_{n=0}^{\infty}\left(\frac{2n+1}{2}\int_0^{\pi/2}\times P_n(\cos\alpha)\cos(\alpha)\sin(\alpha)d\alpha\right)P_n(\cos\theta). \tag{6}$$

The second member in Eq. (6) represents the incident thermal flux, whose value is $(I_o\cos\theta)/2$ for $0 \leqslant \theta \leqslant \pi/2$, and 0 for all other angles [see Fig. 1(b)], after being expanded in Legendre series.[6] Substituting Eq. (5) into Eq. (6) the temperature of the sphere is obtained

$$T(r,\theta,\omega)=\frac{I_o}{2Kq}\sum_{n=0}^{\infty}\left(\frac{2n+1}{2}\int_0^{\pi/2}\times P_n(\cos\alpha)\cos(\alpha)\sin(\alpha)d\alpha\right)\frac{j_n(qr)P_n(\cos\theta)}{j'_n(qa)+Rj_n(qa)}, \tag{7}$$

where j'_n are the derivatives of the spherical Bessel.

Equations (4), (3), and (7) allow us to calculate the temperature oscillation at any point of a solid cylinder, a hollow cylinder and a sphere whose surfaces are periodically illuminated, respectively. Then, using the inverse Laplace transform, the temperature evolution after the absorption of a light pulse can be calculated.[7] Following this procedure, the temperature rise of the rear surface of four stainless steel samples ($K=14.5$ W m^{-1} K^{-1}, $D=3.7$ mm^2 s^{-1}) after the absorption of a Dirac pulse has been simulated: (a) a 3 mm-thick slab, i.e., the classical configuration for the flash method; (b) a solid cylinder of 3 mm in diameter whose temperature is measured at the bottom pole, $\phi=-\pi/2$; (c) a solid sphere of 3 mm in diameter whose temperature is measured at $\theta=\pi$ and (d) a hollow cylinder with an outer diameter of 3 mm and an inner diameter of 2 mm, whose temperature is measured at $\phi=-\pi/2$. Their temperature histories are shown in Fig. 2(a) for negligible heat losses ($h=h'=0$). For each sample, the temperature has been normalized to the asymptotic value at long times. Calculations performed for a wide variety of material properties indicate that the time required by the back surface to reach the half of the maximum

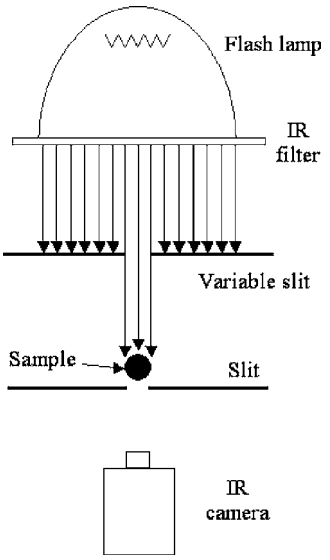

FIG. 3. Experimental setup.

temperature rise ($t_{1/2}$) only depends on the thermal diffusivity and on the sample size, through the equation

$$t_{1/2} = A\frac{d^2}{D}, \tag{8}$$

where d is the thickness in the case of a slab or the diameter ($2a$) in the case of a solid cylinder and a solid sphere. For slabs, A is the well-known 0.1388,[1] while for solid cylinders and spheres, we found $A=0.1068$ and $A=0.08840$, respectively. A simple formula has not been encountered for hollow cylinders.

The influence of heat losses is shown in Fig. 2(b), where calculations have been performed with $h=200$ W m^{-2} K^{-1} and $h'=100$ W m^{-2} K^{-1}. Note that for the same h value the effect of heat losses in the temperature evolution increases as we change from slabs to solid cylinders and to solid spheres, the highest one being for hollow cylinders. This is due to the fact that heat losses are proportional to the surface from which heat is transferred, provided the same material is considered.

The validity of the theory has been tested experimentally by measuring the following AISI-304 stainless steel samples: A rod whose diameter is 4 mm, a hollow cylinder with an outer diameter of 2.05 mm and an inner diameter of 1.55 mm, and a 2 mm thick plate that has been used as a reference. Measurements have been performed by an infrared thermography setup whose scheme is shown in Fig. 3. The samples have been illuminated by a 6 kJ flash lamp and their rear surface temperature has been measured by an infrared camera (Thermacam SC 2000 from FLIR Systems) with a focal plane array of 320×240 pixels working in the $8-12$ μm spectral range at a frequency rate of 50 frames per second. An infrared filter in front of the flash lamp is used to cut its infrared emission. A variable slit is placed between the lamp and the sample. Its width is fitted to the sample diameter in order to guarantee uniform illumination of the sample. A second slit is placed between the sample and the infrared camera in order to prevent direct light from reaching the detector. When using a Ge lens with a field of view of $24°\times18°$ together with a close-up lens, the minimum working distance is 10 cm, allowing us to sample a rectangle as small as 4.4 cm$\times$3.1 cm. This means that each pixel measures the average temperature over a square on the sample of 0.14 mm in side. Therefore, for rods of 4 mm and 2 mm in diameter, the pixel that corresponds to the center of the cylinder does not measure the temperature just at $\phi=-\pi/2$, but the average temperature over a sector of 4° and 8°, respectively. Theoretical calculations of the average temperature over such sectors indicate that the error in the thermal diffusivity is less than 0.5%.

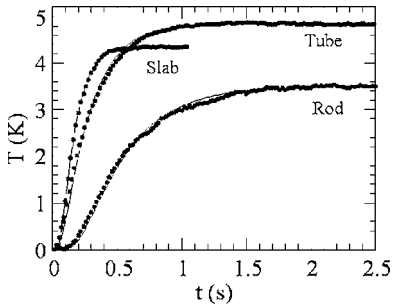

FIG. 4. Temperature rise with respect to the ambient versus time after the absorption of a flash light. Dots are experimental points and the continuous lines are the fit to the theoretical models.

In Fig. 4, the temperature rise with respect to the ambient after the flash light for the three samples under study is shown by dots. In the case of the two cylindrical samples, the temperature is the average of 100 pixels placed along the cylinder axis. In the three cases, the temperature reaches a constant value at long times after the flash light, indicating that the influence of heat losses is negligible. Using Eq. (8) $D=3.76\pm0.10$ mm^2/s and $D=3.70\pm0.14$ mm^2/s are obtained for the slab and the rod, respectively. The error is the standard deviation over 10 measurements performed in each sample. The continuous lines in Fig. 4 are the fit to the theoretical model, i.e., to Eq. (3) for the tube, to Eq. (4) for the rod, and to Eq. (3) in Ref. 1 for the slab. The fitted thermal diffusivity of the tube is 3.84 ± 0.16 mm^2/s; while for the slab and for the rod, the same thermal diffusivity values as those found using Eq. (8) are obtained. All values are consistent and fall inside the typical thermal diffusivity values of AISI-304 that can be found in the literature (3.7–4.0 mm^2/s).

This work has been supported by the MCyT (MAT2002-04153-C02-01) and by the MEC (MAT2005-02999).

[1] W. J. Parker, R. J. Jenkins, C. P. Butler, and G. L. Abbott, J. Appl. Phys. **32**, 1679 (1961).
[2] C. Wang, A. Mandelis, and Y. Liu, J. Appl. Phys. **96**, 3756 (2004).
[3] C. Wang, A. Mandelis, and Y. Liu, J. Appl. Phys. **97**, 014911 (2005).
[4] J. Sinai and R. C. Waag, J. Acoust. Soc. Am. **83**, 1729 (1988).
[5] N. B. Kakogiannos and J. A. Roumeliotis, J. Acoust. Soc. Am. **98**, 3508 (1995).
[6] G. Arfken, *Mathematical Methods for Physicists* (Academic, Orlando, 1985), p. 654.
[7] J. C. Krapez, J. Appl. Phys. **87**, 4514 (2000).